Tuning and stability of a singly resonant continuous-wave optical parametric oscillator close to degeneracy

Markku Vainio,[1,2,*] Cécile Ozanam,[1,3] Ville Ulvila,[1] and Lauri Halonen[1]

[1]*Laboratory of Physical Chemistry, Department of Chemistry, P.O. Box 55 (A.I. Virtasen aukio 1), FIN-00014, University of Helsinki, Finland*
[2]*Centre for Metrology and Accreditation, P.O. Box 9, FIN-02151 Espoo, Finland*
[3]*École Polytechnique (member of ParisTech), F-91128 Palaiseau Cedex, France*
**markku.vainio@helsinki.fi*

Abstract: Wavelength tuning and stability characteristics of a singly resonant continuous-wave optical parametric oscillator (cw OPO) in the proximity of signal-idler degeneracy have been studied. The OPO is made singly resonant by using a Bragg grating as a spectral filter in the OPO cavity. The signal-idler frequency difference can be tuned from 0.5 to 7 THz, which makes the OPO suitable for cw THz generation by optical heterodyning. The operation of the OPO within this singly-resonant regime is characterized by a strong self-stabilization effect. A gradual transition to an unstable, doubly-resonant regime is observed for a signal-idler detuning smaller than ~0.5 THz.

OCIS codes: (190.4410) Nonlinear optics, parametric processes; (190.4970) Parametric oscillators and amplifiers; (140.6810) Thermal effects.

References and links

1. K. L. Vodopyanov, E. Sorokin, I. T. Sorokina, and P. G. Schunemann, "Mid-IR frequency comb source spanning 4.4-5.4 μm based on subharmonic GaAs optical parametric oscillator," Opt. Lett. **36**(12), 2275–2277 (2011).
2. J. E. Schaar, K. L. Vodopyanov, and M. M. Fejer, "Intracavity terahertz-wave generation in a synchronously pumped optical parametric oscillator using quasi-phase-matched GaAs," Opt. Lett. **32**(10), 1284–1286 (2007).
3. M. E. Marhic, K. K. Y. Wong, L. G. Kazovsky, and T. E. Tsai, "Continuous-wave fiber optical parametric oscillator," Opt. Lett. **27**(16), 1439–1441 (2002).
4. S. T. Yang, R. C. Eckardt, and R. L. Byer, "Power and spectral characteristics of continuous-wave parametric oscillators: the doubly to singly resonant transition," J. Opt. Soc. Am. B **10**(9), 1684–1695 (1993).
5. A. J. Henderson, M. J. Padgett, F. G. Colville, J. Zhang, and M. H. Dunn, "Doubly-resonant optical parametric oscillators: tuning behaviour and stability requirements," Opt. Commun. **119**(1-2), 256–264 (1995).
6. M. Vainio and L. Halonen, "Stable operation of a cw optical parametric oscillator near the signal-idler degeneracy," Opt. Lett. **36**(4), 475–477 (2011).
7. J. Saikawa, M. Fujii, H. Ishizuki, and T. Taira, "High-energy, narrow-bandwidth periodically poled Mg-doped $LiNbO_3$ optical parametric oscillator with a volume Bragg grating," Opt. Lett. **32**(20), 2996–2998 (2007).
8. B. Jacobsson, V. Pasiskevicius, F. Laurell, E. Rotari, V. Smirnov, and L. Glebov, "Tunable narrowband optical parametric oscillator using a transversely chirped Bragg grating," Opt. Lett. **34**(4), 449–451 (2009).
9. O. Gayer, Z. Sacks, E. Galun, and A. Arie, "Temperature and wavelength dependent refractive index equations for MgO-doped congruent and stoichiometric $LiNbO_3$," Appl. Phys. B **91**(2), 343–348 (2008).
10. O. Paul, A. Quosig, T. Bauer, M. Nittmann, J. Bartschke, G. Anstett, and J. A. L'huillier, "Temperature-dependent Sellemeier equation in the MIR for the extraordinary refractive index of 5% MgO doped congruent $LiNbO_3$," Appl. Phys. B **86**(1), 111–115 (2006).
11. S. T. Lin, Y. Y. Lin, T. D. Wang, and Y. C. Huang, "Thermal waveguide OPO," Opt. Express **18**(2), 1323–1329 (2010), http://www.opticsinfobase.org/abstract.cfm?URI=oe-18-2-1323.
12. M. Vainio, J. Peltola, S. Persijn, F. J. M. Harren, and L. Halonen, "Thermal effects in singly resonant continuous-wave optical parametric oscillators," Appl. Phys. B **94**(3), 411–427 (2009).
13. A. Godard, M. Raybaut, T. Schmid, M. Lefebvre, A.-M. Michel, and M. Péalat, "Management of thermal effects in high-repetition-rate pulsed optical parametric oscillators," Opt. Lett. **35**(21), 3667–3669 (2010).
14. A. J. Henderson and R. Stafford, "Intra-cavity power effects in singly resonant cw OPOs," Appl. Phys. B **85**(2-3), 181–184 (2006).
15. P. L. Hansen and P. Buchhave, "Thermal self-frequency locking of a doubly resonant optical parametric oscillator," Opt. Lett. **22**(14), 1074–1076 (1997).

#153839 - $15.00 USD Received 31 Aug 2011; revised 5 Oct 2011; accepted 5 Oct 2011; published 25 Oct 2011

16. T. Ikegami, S. Slyusarev, T. Kurosu, Y. Fukuyama, and S. Ohshima, "Characteristics of a cw monolithic optical parametric oscillator," Appl. Phys. B **66**(6), 719–725 (1998).
17. A. Douillet, J.-J. Zondy, A. Yelisseyev, S. Lobanov, and L. Isaenko, "Stability and frequency tuning of thermally loaded continuous-wave $AgGaS_2$ optical parametric oscillators," J. Opt. Soc. Am. B **16**(9), 1481–1498 (1999).
18. J.-J. Zondy, A. Douillet, A. Clairon, A. Yelisseyev, L. Isaenko, and S. Lobanov, "Thermal effects limitations in mid-infrared continuous wave optical parametric oscillators," J. Mater. Sci. Mater. Electron. **12**(8), 451–460 (2001).
19. N. P. Barnes and J. A. Williams-Byrd, "Average power effects in parametric oscillators and amplifiers," J. Opt. Soc. Am. B **12**(1), 124–131 (1995).
20. T. Ikegami, S. Slyusarev, and S.-I. Ohshimal, "Long-term, mode-hop-free operation of a continuous-wave, doubly resonant, monolithic optical parametric oscillator," Opt. Commun. **184**(1-4), 13–17 (2000).
21. J. E. Hellström, B. Jacobsson, V. Pasiskevicius, and F. Laurell, "Finite beams in reflective volume Bragg gratings: theory and experiments," IEEE J. Quantum Electron. **44**(1), 81–89 (2008).
22. S. Schiller, J. Schoser, C. Braxmaier, K. Bencheikh, U. Strössner, A. Peters, J. Mlynek, and P. De Natale, "Single-frequency CW optical parametric oscillators: devices and applications," in *Proc. Int. Conf. Laser Spectroscopy XIV*, R. Blatt, ed. (World Scientific Publishing, Singapore, 1999), pp. 217–226.
23. T. Waritanant and T.-y. Chung, "Influence of minute self-absorption of a volume Bragg grating used as a laser mirror," IEEE J. Quantum Electron. **47**(3), 390–397 (2011).
24. M. Vainio, M. Siltanen, J. Peltola, and L. Halonen, "Grating-cavity continuous-wave optical parametric oscillators for high-resolution mid-infrared spectroscopy," Appl. Opt. **50**(4), A1–A10 (2011).
25. S. Tjörnhammar, B. Jacobsson, V. Pasiskevicius, and F. Laurell, "Thermal limitations of volume Bragg gratings when used in lasers for spectral control," in *Proceedings of 2nd EOS Topical Meeting on Lasers ETML'11* (European Optical Society, 2011), paper 4609.

1. Introduction

Optical parametric oscillators (OPOs) operated at or near degeneracy, i.e. so that the signal (ν_s) and idler (ν_i) frequencies are nearly equal to each other and half of the pump frequency (ν_p), have some interesting properties that can be advantageous in various applications. The parametric gain bandwidth of a near-degenerate OPO is typically large, which is useful for generation of short mid-infrared pulses and mid-infrared supercontinua [1]. Another interesting application is the generation of a pair of coherent beams (signal and idler), whose frequency difference is in the THz region. Such a dual-frequency source can be used for THz wave generation by optical heterodyning [2]. Pulsed near-degenerate OPOs have been extensively studied both from the fundamental and applied point of view, but the continuous-wave (cw) regime is less explored. Most of the previous work with cw sources has been done with OPOs based on optical fibers or waveguides, in which case the main motivation for near-degenerate operation is simplification of the instrument fabrication and the intrinsic reduction of the oscillation threshold when approaching degeneracy [3].

A major complication in obtaining stable near-degenerate operation of a bulk OPO is that the OPO easily becomes doubly resonant. This is due to the difficulty of getting mirrors that are highly reflective for only one of the two wavelengths, signal or idler, while transmitting the other. The doubly resonant OPO (DRO) has a lower threshold than the singly resonant OPO (SRO), but it usually requires active control of the cavity length and tends to be more unstable [4, 5]. Spectral instabilities are particularly prominent close to degeneracy, where the OPO becomes highly sensitive to fluctuations of the operating parameters, such as the pump wavelength and crystal temperature [5, 6]. Spectral characteristics of a near-degenerate OPO can be improved by placing a narrow-band spectral filter in the OPO cavity, so that singly resonant operation is maintained even close to degeneracy [7,8]. We have recently demonstrated that, by using a Bragg grating as the spectral filter, this technique can provide stable operation in a single longitudinal mode of the OPO cavity [6]. Additional benefits of the grating-stabilized OPO are that the signal-idler frequency difference can be tuned over several THz, and that the stable output power of the SRO is typically an order of magnitude higher than that of the DRO.

In this paper, we report a wide tuning range and high output power of a near-degenerate cw SRO, which is based on a Bragg grating. We present a detailed experimental study of the tuning and stability characteristics of the SRO close to degeneracy. These two characteristics are of uttermost importance in practical applications, such as in cw THz generation. In particular, we report an observation of strong self-stabilization of the SRO, which helps to

#153839 - $15.00 USD Received 31 Aug 2011; revised 5 Oct 2011; accepted 5 Oct 2011; published 25 Oct 2011

maintain single mode operation and makes the SRO insensitive to disturbances in the pump frequency and power. Finally, we discuss the transition from singly to doubly resonant regime when the frequency detuning from degeneracy becomes comparable to the reflection bandwidth of the Bragg grating.

2. Experimental setup

A comparison of the singly resonant near-degenerate continuous-wave OPO with a conventional near-degenerate OPO has been given in our previous publication [6]. The singly resonant OPO is schematically shown in Fig. 1. The OPO cavity is a bow-tie ring cavity that comprises three mirrors and a reflective Bragg grating. The mirrors are highly reflective for both signal and idler beams, but the Bragg grating reflects only one of the wavelengths and makes the cavity singly resonant. In this paper, we term the resonant wave signal, and the nonresonant wave idler. Although not unambiguous upon the transition to DRO, this definition avoids confusion when we present results that demonstrate tuning across the degeneracy point. In most of the experiments reported here, the resonant frequency is higher than the nonresonant frequency, in which case the definition is consistent with the customary notation $\nu_s > \nu_i$.

The 1.6 mm thick Bragg grating has been recorded in a bulk of photosensitive glass using a volume holographic technique. The peak reflectivity of the grating is ~98.5%, the center wavelength at 7° angle of incidence is ~1584.5 nm, and the reflection bandwidth stated by the manufacturer (OptiGrate Corp., USA) is 130 GHz (FWHM). The grating transmits approximately 1% of the signal power resonating in the OPO cavity. The power of the nonresonant idler beam is almost completely transmitted. Only a small outcoupling loss of ~1% is caused by residual reflections at the antireflection coated surfaces of the grating substrate. A small slant between the grating and the substrate prevents the residual reflections from coupling back to the OPO cavity.

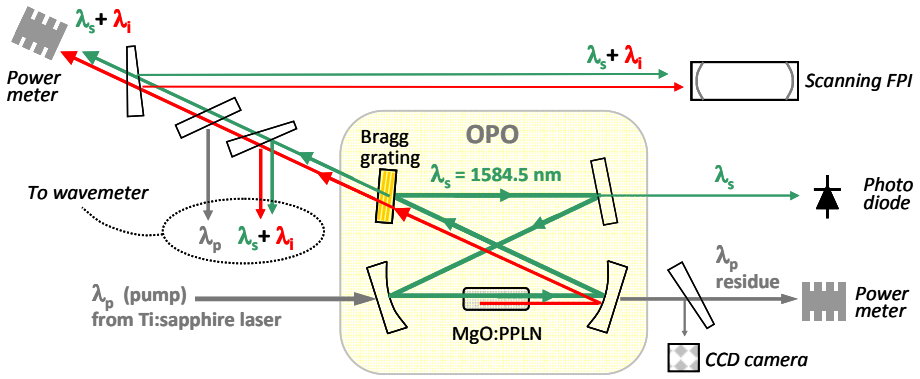

Fig. 1. Schematic of the OPO and the measurement setup. The folding angle of the OPO cavity is 7 degrees.

The total length of the OPO cavity is 0.7 m, which corresponds to a free spectral range (FSR) of 430 MHz. The cavity was designed so that the $1/e^2$ radius of the waist of the resonant beam in the nonlinear crystal is 50 µm. The spot radius at the Bragg grating is 370 µm. The OPO is pumped with a wavelength-tunable cw Ti:sapphire laser (MBR-PS, Coherent Inc., USA) at ~800 nm, which sets the degeneracy wavelength to about 1.6 µm. The pump beam, which passes the nonlinear crystal once, is mode matched to the signal beam so that the confocal parameters of the two beams are equal to each other. The nonlinear crystal is a 50-mm long, 0.5-mm thick, 5% MgO-doped periodically poled lithium niobate, MgO:PPLN (HC Photonics Corp., Taiwan). It has ten adjacent poling periods, three of which (Λ = 20.3, 20.5, and 20.7 µm) were used in the work reported here. The end facets of the crystal are

#153839 - $15.00 USD Received 31 Aug 2011; revised 5 Oct 2011; accepted 5 Oct 2011; published 25 Oct 2011

antireflection coated for the pump, signal, and idler. The residual reflectivity of a coated facet is <0.25% for the wavelength resonating in the OPO cavity. Temperature of the crystal is controlled with 20 mK stability using Peltier elements. The OPO cavity is not thermally stabilized, but it is shielded from air fluctuations by a hardboard cover.

Figure 1 shows the main components of the optical instrumentation that was used to characterize the performance of the OPO. Pump power was measured after the OPO, and the corresponding power in the MgO:PPLN crystal was calculated using calibrated transmission of the OPO mirrors at the pump wavelength. The mirrors were not designed for this particular setup, and therefore transmit only ~60% of the pump power, depending on the pump wavelength. The use of the Bragg grating guarantees that the pump beam does not resonate in the OPO cavity. The pump wavelength was monitored with a wavelength meter (EXFO WA-1500). The total output power of the OPO was measured behind the Bragg grating, after filtering out the residue of the pump beam. A small fraction of the output beam was taken to a wavelength meter (EXFO WA-1500), which together with a Fourier-transform spectrum analyzer (EXFO WA-650) was used to monitor the OPO spectrum. In addition, a scanning Fabry-Pérot interferometer (FPI) was used to study the spectral characteristics of the signal and idler beams in more detail. A high-speed InGaAs photodiode (Thorlabs DET410) placed after the flat OPO cavity mirror allowed us to observe fast power fluctuations of the resonant beam(s). The spatial profile of the undepleted pump beam was monitored after the OPO cavity using a CCD camera.

3. Wavelength tuning close to degeneracy

3.1 Tuning range

The wavelength of the Bragg-grating-stabilized near-degenerate OPO can be scanned by tuning the pump laser wavelength λ_p, and by synchronously adjusting the temperature of the nonlinear crystal so that the phase matching condition remains fulfilled [6]. The scanning of the pump frequency is entirely transferred to the idler frequency ($\nu_i = \nu_p - \nu_s$) because the signal wavelength is fixed by the grating. Figure 2a demonstrates this tuning method in terms of the signal-idler frequency difference $\nu_s - \nu_i$ and as a function of crystal temperature. The phase matching relationship between the pump wavelength and crystal temperature is plotted in Fig. 2b.

The frequency difference $\nu_s - \nu_i$ can be tuned to any value between 0.5 and 7 THz. At the low-frequency side, the tuning range is limited by spectral instabilities that arise due to the transition from singly to doubly resonant OPO. This interesting region, which is indicated in gray in Fig. 2a, is discussed in more detail in Section 4. The maximum frequency difference that our present setup can produce is 7 THz. This is not a fundamental limit but a consequence of nonoptimized cavity mirrors that prevent us from obtaining sufficient pump power into the OPO crystal at $\lambda_p > 808$ nm.

Mode-hop-free fine tuning of $\nu_s - \nu_i$ over 20 GHz is obtained at each temperature set point by scanning the pump laser. The maximum total tuning that can be done by mere pump tuning is approximately 60 GHz, depending on the width of the parametric gain curve at the operating point, i.e., depending on the pump level and detuning from degeneracy [6].

#153839 - $15.00 USD Received 31 Aug 2011; revised 5 Oct 2011; accepted 5 Oct 2011; published 25 Oct 2011

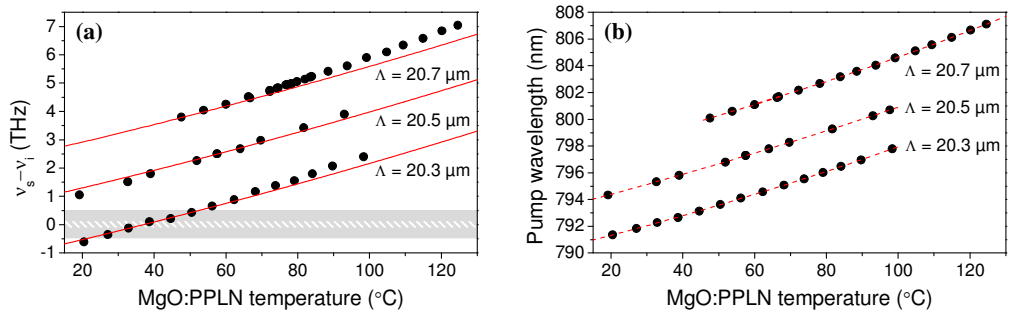

Fig. 2. (a) Tuning of the signal-idler frequency difference as a function of crystal temperature for different poling periods Λ. Dots are measured points and solid lines are theoretical phase matching curves calculated using the Sellmeier data from [9] without taking into account thermal dephasing. Thermal expansion of the crystal was accounted for after [10]. The gray area indicates transition from SRO to DRO, and the dashed area shows the DRO regime. (b) Phase-matched pump wavelength as a function crystal temperature, when the resonant signal wavelength of the OPO is fixed to ~1584.5 nm. The dashed lines are guides to the eye.

3.2 Output power

The maximum total output power of the OPO exceeds 0.5 W within the entire SRO tuning range plotted in Fig. 2. This consists of both signal and idler power. The exact ratio of the two powers depends on the reflectivity of the Bragg grating, which in turn depends on the grating angle, as well as on the exact wavelength of the resonant beam. The reflection bandwidth (130 GHz) of the grating is large compared to the free spectral range (0.43 GHz) of the OPO cavity, and the OPO does not necessarily resonate exactly at the wavelength of the peak reflectivity. With the operating conditions used in the experiments reported here, the non-resonant idler power is approximately 3 times higher than the outleaking fraction of the resonant signal power. In the middle of the wavelength tuning range, where the available pump power is highest, the oscillation threshold is reached at approximately 1.2 W of pump power in the MgO:PPLN crystal, and the output power is up to 1.4 W with 2.6 W pump power. The maximum pump depletion is 70 to 80%.

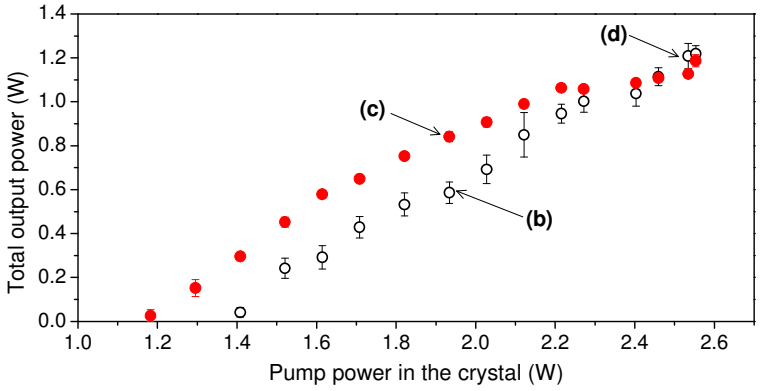

Fig. 3. Total output power (signal + idler) of the SRO at $\nu_s - \nu_i$ ~2.6 THz. Empty dots denote the points measured with increasing pump power. The solid red dots denote the points that were measured when the pump power was decreased from the maximum back to the OPO threshold. Depleted pump beam profiles are presented in Fig. 4 for points (b), (c), and (d).

We measured the OPO output power as a function of pump power first when increasing the pump power and then when decreasing it. The results of these measurements are shown in Fig. 3. When increasing the pump power, the points were measured so that the OPO

#153839 - $15.00 USD Received 31 Aug 2011; revised 5 Oct 2011; accepted 5 Oct 2011; published 25 Oct 2011

oscillation was momentarily blocked after measuring each point. This procedure made it possible for us to check the pump depletion. The error bars of these measurements therefore give indication of the OPO power fluctuation during the first 30 - 60 s after the onset of OPO oscillation (i.e., after unblocking the resonant beam). Despite the larger power fluctuation, this procedure did not change the observed average power levels compared to the case where the pump power was increased without blocking the beam between the measurements. For the measurement done with decreasing the pump power, the OPO was running continuously during the entire measurement. The only parameter that was varied was the pump power. In this case, the observed output power is more stable, even immediately after changing the pump power. If the OPO oscillation is blocked between the measurements, the output power levels are the same as for the measurement with increasing pump power.

The hysteresis in the power curves in terms of the direction of the power change suggests that the OPO is affected by thermal lensing [11,12] and/or axial temperature gradient [13]. To study this in more detail, we reduced the thermal load in the MgO:PPLN crystal by chopping the signal beam that resonates in the OPO cavity. The chopping frequency and duty cycle were 5 Hz and 50%, respectively. The power curve measured in the chopped mode was similar to that measured in the true cw mode when increasing the pump power. The same power curve was also observed when chopping the pump beam instead of the signal beam. Although these tests did not indicate presence of thermal effect due to absorption of any of the three beams, weak thermal lensing caused by the resonating signal beam was verified by observing the spatial profile of the pump beam behind the OPO with a CCD camera (Fig. 4). As expected, thermal lensing was noticed to be strongest in the narrow (0.5 mm) dimension of the crystal. These observations confirm that thermal lensing in the crystal is so weak that it does not limit the OPO conversion efficiency at high powers. Thermal lensing is subtle, and the evolution of the pump beam profile behind the OPO versus pump power reveals no indication of thermal waveguiding [11]. This is as expected, considering the low intracavity power (estimated to be <50 W at the maximum pump power) and the small absorption coefficient of MgO:PPLN at the resonant wavelength [12,14].

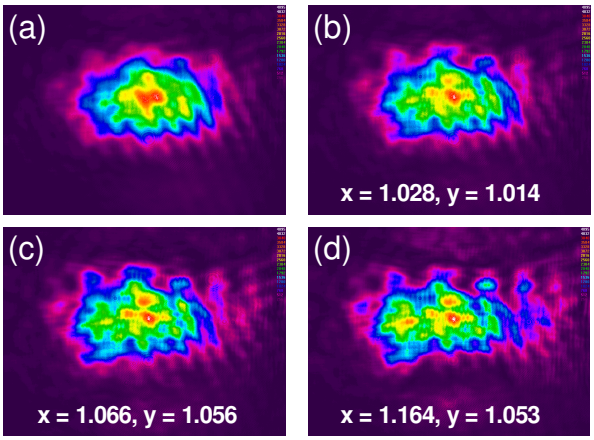

Fig. 4. Pump beam profile measured after the OPO. Panel (a) shows the undepleted pump beam (OPO blocked) at the maximum pump power. Panels (b) to (d) show the depleted pump beam at respective points of Fig. 3. The $1/e^2$-diameter of the beam in x (horizontal) and y (vertical) directions are given as normalized to the respective diameters of the undepleted pump beam shown in panel (a). Horizontal (x) direction is the direction of narrow dimension of the MgO:PPLN crystal.

#153839 - $15.00 USD Received 31 Aug 2011; revised 5 Oct 2011; accepted 5 Oct 2011; published 25 Oct 2011

3.3 Thermal dephasing and self-locking

Although thermal lensing is modest in our OPO, the effect of dephasing due to self-induced heating in the crystal is pronounced. As a first indication of thermal dephasing, we observed that, at the maximum output power, the set temperature of the MgO:PPLN crystal that gives the optimum phase matching is 0.5°C higher in the chopped mode than in the true cw mode. We studied this effect in more detail by monitoring the OPO power with a fast photodiode while applying a linear scan to the crystal temperature. The results of these measurements are shown in Figs. 5a–5c for different scan speeds and directions. The scans with decreasing temperature are plotted in blue, and those with increasing temperature are plotted in red. As is clear from the figure, the temperature range over which parametric oscillation is sustained is conspicuously different for different scan directions. In addition, the tuning speed over the OPO cavity modes is different on different sides of the gain profile, which is seen as a variation of the fine structure of the bell-shaped curves. These asymmetries are typical signs of thermal self-locking, which is a well known phenomenon in doubly and triply resonant OPOs [15–18], and has also been observed in SROs [12].

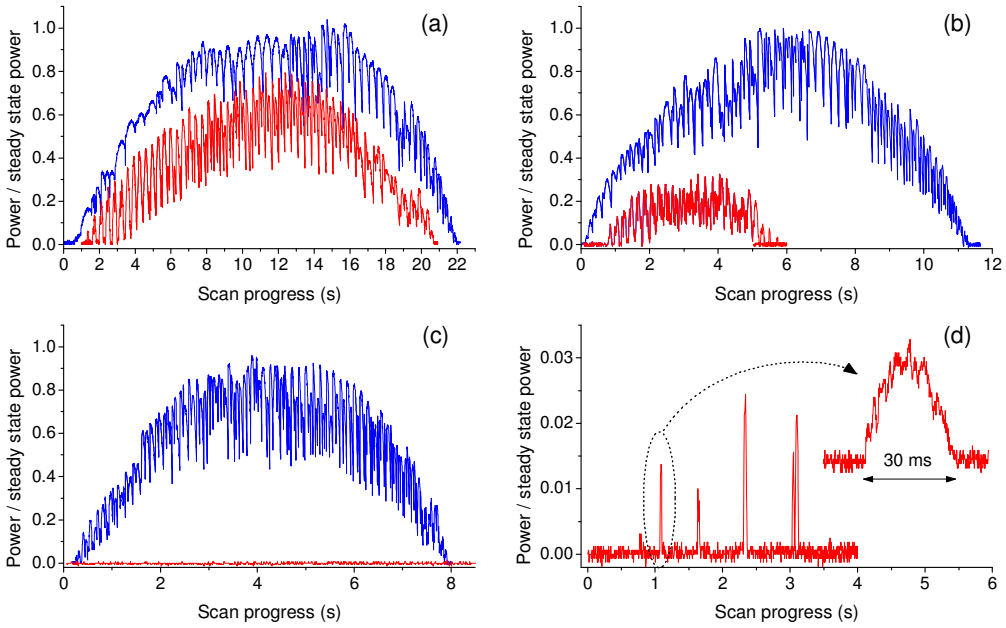

Fig. 5. SRO output power during MgO:PPLN temperature scanning. The scan speeds are (a) 0.14 K/s, (b) 0.28 K/s, and (c) 0.42 K/s. Note the different time scales of the horizontal axes. The blue wide curves indicate temperature scans for decreasing temperature, and the red curves for increasing temperature. The power is normalized to the steady state output power, which is 1.4 W (at Λ = 20.5 µm, T = 61.7°C, and ν_s–ν_i ~2.6 THz). (d) Short and weak peaks are observed at scan speed ~0.35 K/s with increasing temperature. One of the peaks is shown in detail in the inset.

The thermal self-locking effect can partly compensate for the disturbances caused by fluctuations in the SRO cavity length, pump frequency, or other operating parameters that would normally lead to a longitudinal mode hop of the OPO. If the detuning between the resonating frequency and the parametric gain curve changes as a result of a disturbance, the power resonating in the OPO cavity changes as well. This change in the power leads to a change of the crystal temperature due to the corresponding variation of the absorbed intracavity power in the crystal (self-heating). Depending on the sign of the detuning between the cavity resonance frequency and the parametric gain curve, this heating/cooling either resists or amplifies the effect of the disturbance. Such a thermo-optic effect is described in detail, e.g., in [17], and it can be qualitatively understood from the results shown in Fig. 5. As

#153839 - $15.00 USD Received 31 Aug 2011; revised 5 Oct 2011; accepted 5 Oct 2011; published 25 Oct 2011

an example, the blue curve of Fig. 5a shows how the OPO is first pushed closer to the parametric gain maximum as the crystal temperature is ramped down. The subsequent build-up of the power resonating in the OPO cavity increases the absorbed power in the crystal, and therefore locally elevates the crystal temperature, partly compensating for the temperature ramping. This leads to self-frequency-locking, which is seen as broadened peaks on the left-hand side of the blue curve. On the other side of the gain maximum (the right-hand side of the blue curve), the self-heating is reduced as the scan progresses, which leads to an accelerated passage through the cavity modes instead of self-locking. The start of the accelerated passage is delayed because under the self-locked operation (left-hand side of the curve) the thermally loaded OPO reaches the peak gain later than it would in the case of a cold cavity.

The red curve of Fig. 5a shows the case where the temperature of the crystal is ramped up. The local temperature change within the beam volume in the crystal is accelerated by the self-heating effect as soon as the OPO oscillation starts. This is seen as increasingly rapid passage over the cavity modes on the left-hand side of the red curve, as the intracavity power becomes higher. Self-heating pushes the OPO across the gain maximum faster than would normally happen without the absorption of the intracavity power in the crystal. This explains why the region of self-locked operation (compensation of temperature ramping by a decrease in self-heating) is narrow and takes place only at the end of the temperature scan.

Thermal self-locking is the dominating effect when the crystal temperature is decreased, and the thermal-accelerated passage dominates when the crystal temperature is ramped up. The difference between the two cases becomes more distinct as the speed of the temperature scan is increased, as is seen from Figs. 5b–5c. The peak output power during the downward scans is nearly independent of the scan speed, and the width of the bell-shaped curve in terms of temperature remains essentially constant, ~3 K. When the temperature is ramped up, the peak power and the temperature acceptance bandwidth get smaller as the scan speed is increased. The radial heat diffusion time, i.e. the time during which the crystal temperature across the beam profile reaches equilibrium in the presence of thermal load, can be calculated to be of the order of a millisecond [19]. This suggests that the fastest passage time over a cavity resonance at high scan speeds should be of the same order of magnitude. The shortest peaks we were able to observe were 20-30 ms (Fig. 5d). However, it seems that during this time the OPO jumps over several cavity modes. It could also be that even shorter and weaker peaks exist but they are just beyond the detection limit of our measurement setup.

The self-locking effect has some practical consequences. First, a set point of the crystal temperature for which the OPO oscillates with a certain pump wavelength is easy to find if the temperature is decreased, but not when it is increased. Second, the self-locking effect can significantly help to suppress mode hops and hence to improve the frequency stability of the OPO [16–18,20]. This important property is discussed in subsection 4.2.

4. Stability characteristics close to degeneracy

4.1 Transition between the singly and doubly resonant OPO

The OPO is singly resonant and oscillates on a single longitudinal mode of the cavity for any signal-idler frequency difference larger than 0.5 THz. Single-mode operation is maintained even at the highest available pump level, which is 2.3 times the SRO threshold. This was confirmed both by monitoring the output power of the resonant beam with an InGaAs photodiode, and by looking at the output spectrum with a Fabry-Pérot interferometer (Fig. 6a). As the signal-idler detuning becomes smaller than 0.5 THz and comparable to the reflection bandwidth of the Bragg grating, we observe a gradual transition from singly to doubly resonant operation. (Note that the parametric gain bandwidth this close to degeneracy is several THz, which is much larger than the FWHM reflection bandwidth of the grating [6].) This transition is demonstrated in Figs. 6b and 6c that show the output power and FPI plots of the OPO for $\nu_s - \nu_i = 0.15$ THz and $\nu_s - \nu_i < 0.1$ THz, respectively. In Fig. 6b, the output power varies between a few discrete states but does not go to zero. This behavior is similar to that reported earlier by Yang *et al*., and indicates operation in a region where the nominally

#153839 - $15.00 USD Received 31 Aug 2011; revised 5 Oct 2011; accepted 5 Oct 2011; published 25 Oct 2011

nonresonant idler wave becomes weakly resonant [4]. The amplitude and period of the power variations depend on the operating point and conditions. Two different examples are shown in Fig. 6b (left panel). The different power levels correspond to different modes of the OPO cavity, and multimode operation is observed in the FPI spectrum. In many cases, the spectral content remains stable over several seconds despite the strong power fluctuations.

Clear doubly resonant operation is observed at $\nu_s - \nu_i < 0.1$ THz. This is evidenced in Fig. 6c (left panel) by the sections where the OPO output power drops to zero. Mode hopping was observed also in this case, but the rate of hopping was such that only one or few peaks were observed during a single 12 ms long scan of the FPI (Fig. 6c, right panel).

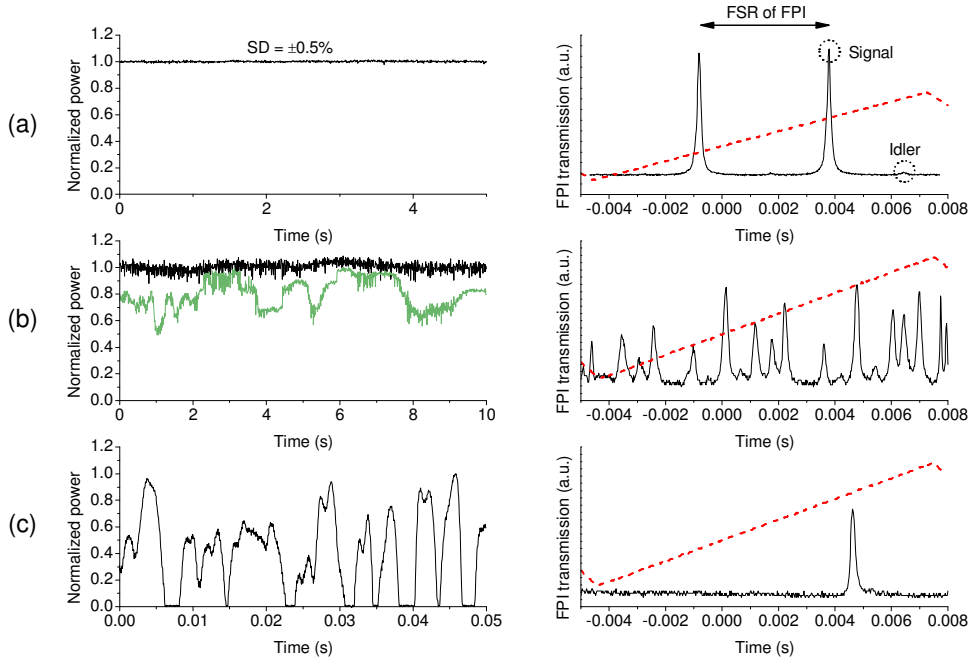

Fig. 6. Transition between the SRO and DRO. Left column shows the normalized signal output powers and the right column shows the corresponding FPI spectra. The red dashed curves indicate the scan signals applied to the FPI. (a) Stable SRO with $\nu_s - \nu_i$ ~1 THz. (b) Weakly DRO with $\nu_s - \nu_i$ ~0.15 THz. (c) DRO with $\nu_s - \nu_i < 0.1$ THz. The pump power in the MgO:PPLN crystal was >1.7 W in all measurements. The idler peak in (a) is much weaker than the signal peak owing to the poor finesse of the FPI at the idler wavelength 1594 nm.

The transition between the singly and doubly resonant regimes can be seen in the OPO threshold power, which is plotted as a function of signal-idler detuning in Fig. 7. The threshold is >0.8W for pure SRO operation and drops to a few tens of milliwatts for the DRO. Although the exact detuning from degeneracy where the transition between the SRO and DRO takes place depends on the operating conditions, we have observed some asymmetry in the OPO stability with respect to the degeneracy point. The OPO stability starts to become worse typically at ~0.5 THz for positive detuning of $\nu_s - \nu_i$, but for negative detuning stable operation is often observed until $\nu_s - \nu_i = -0.3$ THz. This is attributed to the asymmetry of the reflection spectrum of the Bragg grating. Such asymmetry can stem from the divergence of the beam(s) incident on the grating, as is discussed in detail in [21]. Briefly, the asymmetry can be understood by considering the beam as a composition of plane waves, whose wavevectors are spread over a small angle that is related with the beam divergence. Each one of these plane waves experiences a different effective reflectivity, since the reflectivity of the Bragg depends on the angle of incidence. Our grating is designed for normal incidence at 1586.9 nm. As the angle of incidence is increased, the wavelength of peak reflectivity is

#153839 - $15.00 USD Received 31 Aug 2011; revised 5 Oct 2011; accepted 5 Oct 2011; published 25 Oct 2011

shifted according to Bragg's law $\lambda = 2dn\sin\theta$, where d is length of the grating period, n is the refractive index, and θ is the angle of incidence in the grating. At the same time, the effective reflectivity drops. The operating angle 7° corresponds to λ_s = 1584.5 nm, so the reflection spectrum of the Bragg grating is leaning towards the long-wavelength side of the resonating wave.

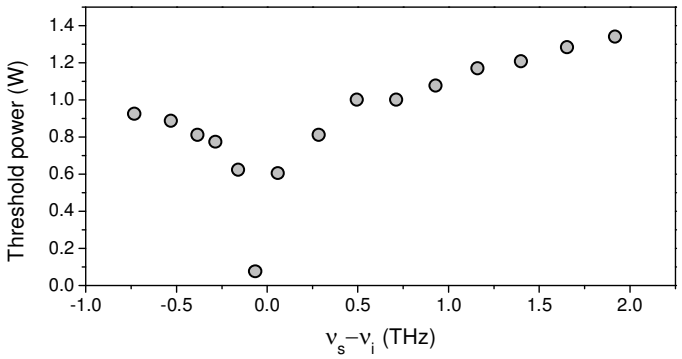

Fig. 7. The OPO threshold power in the MgO:PPLN crystal as a function of signal-idler frequency detuning, measured with Λ = 20.3 μm.

4.2 Long-term stability

The stable singly resonant regime between $\nu_s-\nu_i$ = 0.5 and 7 THz is the most interesting one from the point of view of cw THz generation. We characterized the long term stability of the OPO at $\nu_s-\nu_i$ = 2.6 THz. The measured power and frequency stability of the signal and idler are presented in Fig. 8. Stability of the output power is very good; the standard deviation calculated from the 10-min. measurement shown in Fig. 8 is 0.4%, which is almost equal to the short-term standard deviation calculated from Fig. 6a. The OPO output frequencies, on the other hand, show a linear drift. The drifts of the signal and idler frequencies were observed to be almost equal (20 MHz/min) and to the same direction with each other (Fig. 8). If it were only the OPO cavity that drifted, the drift rates should be the same but the direction of the drift should be the opposite for the signal and idler frequencies since $\nu_p = \nu_s + \nu_i$. The measurement hence indicates that the pump frequency has drifted to the same direction but twice as fast as the signal frequency. This can be explained, e.g., by a frequency drift caused by thermal expansion of the optical cavities due to a change in the laboratory temperature. The relative frequency drift $\Delta\nu/\nu$ of the laser or OPO is equal to the relative change $\Delta L/L$ of the cavity length L. This means that, if the thermal expansion of the two cavities were equally large, the absolute frequency drift of the pump should be twice as large as that of the signal, simply owing to $\nu_p \sim 2\nu_s$.

#153839 - $15.00 USD Received 31 Aug 2011; revised 5 Oct 2011; accepted 5 Oct 2011; published 25 Oct 2011

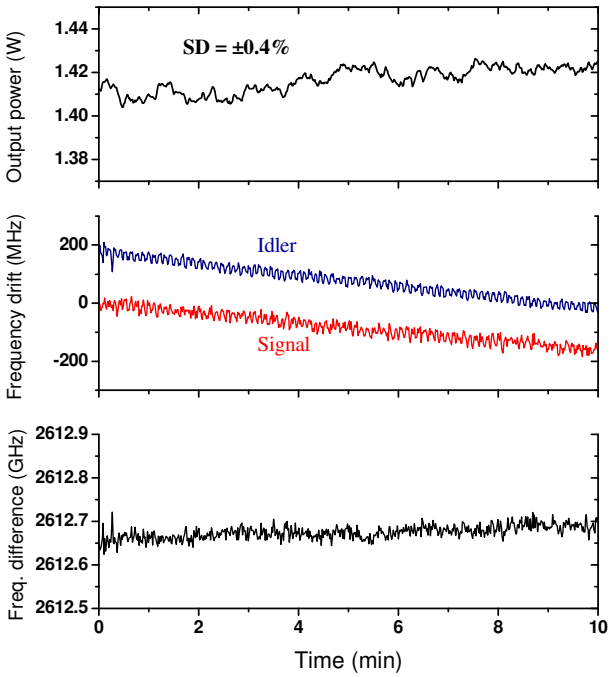

Fig. 8. Stability of the SRO at ν_s–ν_i = 2.6 THz. The upper panel shows the total output power (signal + idler) measured with a power meter that has ~1 s response time. The middle panel shows the drifts of ν_s and ν_i, and the lower panel shows ν_s–ν_i as a function of time. The frequency measurements are limited in short term by the 40 MHz resolution of the wavelength meter.

In principle, it is also possible that the correlation between the drift rates of the pump and signal frequencies is caused by coupling of the two frequencies via the pump power. To rule out the possible coupling, we varied the pump power in steps and monitored the signal beam with the wavelength meter. This is shown in Fig. 9. No change of the signal frequency was observed even with >10% changes in the pump power. Moreover, the OPO is insensitive to mode hops of the pump laser, which are evident as the pump power is changed. These mode hops are seen as jumps in the idler frequency in Fig. 9. Such insensitivity of the OPO to variations of the pump frequency is an intriguing observation, since the standard cold-cavity model (that does not include the effect of thermal load in the OPO resonator) predicts that the SRO should jump from one cavity mode to another whenever the detuning between the resonating cavity mode and the center of the parametric gain exceeds ± 1/2 FSR of the cavity [4,22]. This can easily happen close to degeneracy, where the OPO is extremely sensitive to changes of the pump wavelength. For example, at the operating point ν_s–ν_i = 2.6 THz, the changes in the pump frequency are seen as 200 times larger changes in the phase-matched signal frequency, as can be calculated [6] from the Sellmeier equation and coefficients given in [9]. This means that, on average, a change as small as 1 MHz in the pump frequency should lead to a mode hop of the OPO signal frequency (corresponding to a ½FSR ~215 MHz change in the signal frequency). In striking contradiction with this prediction, no signal mode hop is observed even if the pump frequency changes by up to 2 GHz (Fig. 9).

The sensitivity of the phase-matched signal frequency to the changes of the MgO:PPLN temperature can be estimated in the same manner as the sensitivity to pump frequency [6]. The calculation reveals that a temperature change smaller than 50 μK would be enough to induce a mode hop according to the cold-cavity model. For comparison, the temperature stability of our crystal is ~20 mK. The sensitivity of the phase-matched wavelength to the fluctuations of the operating parameters becomes even stronger the closer one moves to

#153839 - $15.00 USD Received 31 Aug 2011; revised 5 Oct 2011; accepted 5 Oct 2011; published 25 Oct 2011

degeneracy. This can be seen from a typical phase matching curve that shows the phase-matched signal and idler wavelengths as a function of the pump wavelength [6]. It is worth noting that such an increase in the sensitivity of the OPO to the fluctuations of the operating parameters may partly explain the onset of instabilities close to degeneracy, in addition to the already discussed transition from SRO to DRO (Fig. 6b).

It is instructive to compare the characteristics of the near-degenerate SRO with an SRO that operates far from degeneracy. We repeated the above-mentioned calculations for an SRO that is pumped at 1064 nm but resonates at the same wavelength (1584.5 nm) and with the same crystal temperature 62°C (MgO:PPLN, Λ = 30.5 µm) as the near-degenerate SRO discussed in this paper. The calculation shows that the pump frequency of the far-degenerate SRO can be varied by as much as 11 GHz before the phase-matched signal frequency shifts by 215 MHz. The temperature sensitivity of the far-degenerate SRO is reduced by two orders of magnitude compared to the near-degenerate SRO (to ~215 MHz/4.5 mK).

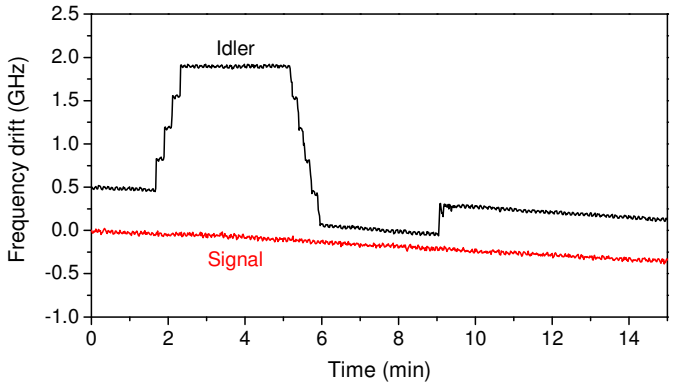

Fig. 9. Stability of the SRO frequencies at ν_s–ν_i = 2.6 THz when the pump laser power is varied. The pump power in the MgO:PPLN crystal is increased stepwise from 2.35 to 2.60 W starting at 2 min., and back to 2.35 W starting at 5 min. A spontaneous mode hop of the pump laser is seen at 9 min.

Considering the high sensitivity of the phase-matched wavelengths to the operation parameters close to degeneracy, the modest spectral filtering provided by the Bragg grating can hardly explain the observed high stability of the OPO. The bandwidth of the Bragg grating reflection spectrum is ~300 times larger than the free spectral range (0.43 GHz) of the SRO cavity and the reflection spectrum is flat close to the wavelength of peak reflectivity [21]. One could therefore expect frequent mode hopping of the OPO signal wave. However, the signal frequency often remains stable without mode hops much longer than the pump frequency does. While the pump laser tends to mode-hop after every 15 minutes or so, the signal frequency often remains in the same longitudinal mode of the OPO cavity for more than half an hour. When a mode hop eventually occurs, the signal frequency typically jumps over several cavity modes. We have observed mode hops larger than 50 GHz, which proves the modest frequency selectivity of the Bragg grating. Moreover, the mode-hop-free drift of the signal frequency can significantly exceed the free spectral range of the cavity, which is in contradiction with the cold-cavity model.

The observed high stability of the SRO is attributed to the thermal self-locking phenomenon discussed in subsection 3.3. The same kind of improvement of the OPO stability owing to thermal self-stabilization has previously been observed in doubly and triply resonant OPOs [16–18,20]. For example, more than 24 h mode-hop-free operation of a DRO without any active stabilization has been reported [20]. We have previously observed that the self-locking effect plays a role in a mid-infrared SRO operated far from degeneracy [12]. However, as was shown above, the SRO operated far from degeneracy is not as sensitive to the fluctuations of the operating parameters as the near-degenerate SRO is. In the near-degenerate SRO discussed here, the self-stabilization effect seems to be essential for long-

#153839 - $15.00 USD Received 31 Aug 2011; revised 5 Oct 2011; accepted 5 Oct 2011; published 25 Oct 2011

term single-mode operation. It is worth pointing out that the same sensitivity of the phase-matched frequency to the crystal temperature that nominally makes the OPO unstable in fact enhances the gain of the thermal self-locking servo [12,17,18].

Finally, it is worth noting that the performance of the volume Bragg grating is also affected by local heating caused by absorption of the intracavity power in the grating [23]. The absorption coefficient for the grating is of the same order of magnitude as for the MgO:PPLN crystal (~10^{-3} cm^{-1}). This leads to a maximum local temperature increase of approximately 1 to 2 K in the grating at the maximum power level of the OPO. The temperature coefficient of the frequency of the grating peak reflectivity is 1.4 GHz/K [24], which is 3 to 4 orders of magnitude smaller than the temperature dependency of phase-matched frequencies in the MgO:PPLN crystal. Therefore, the self-heating in the grating has a negligible effect on the OPO frequency characteristics, and observation of such effect in our OPO is impossible because of other, much stronger effects. For example, if the pump power is varied a lot, or if the OPO operation is blocked and then unblocked again, random shifts of the oscillation frequency up to several tens of GHz can occur. Also any other detrimental effects, such as drop of the grating reflectivity [23,25], due to thermal effects in the Bragg grating are too small to be detected in our setup.

5. Conclusion

We have presented a detailed experimental study of the tuning and stability characteristics of a singly resonant cw OPO close to degeneracy. The OPO is made singly resonant by using a reflective Bragg grating as a cavity mirror. High output power, stable single-mode operation, and wide tuning of the signal-idler frequency difference from 0.5 to 7 THz have been demonstrated. A gradual transition from singly to doubly resonant operation has been observed for signal-idler frequency detuning smaller than ~0.5 THz. Within the transition region, the OPO stability is considerably reduced compared to the singly resonant region.

Despite the sensitivity of the near-degenerate OPO to variations of the operating parameters, such as the pump wavelength, mode-hop-free operation for more than 0.5 h has been observed in the singly resonant regime. This unexpectedly high stability has been attributed to a strong self-stabilization effect, which results from self-heating in the nonlinear crystal due to absorption of the intracavity power of the OPO.

Acknowledgments

M. Vainio, C. Ozanam, and V. Ulvila acknowledge the University of Helsinki for funding the project under which this work was done. M. Vainio thanks the Academy of Finland for financial support.

#153839 - $15.00 USD Received 31 Aug 2011; revised 5 Oct 2011; accepted 5 Oct 2011; published 25 Oct 2011